View metadata, citation and similar papers at core.ac.uk
brought to you by CORE
provided by Elsevier - Publisher Connector

ELSEVIER

Ultrasound in Med. & Biol., Vol. 39, No. 7, pp. 1133–1146, 2013
Copyright © 2013 World Federation for Ultrasound in Medicine & Biology
Printed in the USA. Open access under CC BY-NC-ND license.
0301-5629

http://dx.doi.org/10.1016/j.ultrasmedbio.2013.02.006

● *Review*

ACOUSTIC WAVES IN MEDICAL IMAGING AND DIAGNOSTICS

ARMEN P. SARVAZYAN,* MATTHEW W. URBAN,† and JAMES F. GREENLEAF†

*Artann Laboratories, Trenton, NJ, USA; and †Department of Physiology and Biomedical Engineering, Mayo Clinic College of Medicine, Rochester, MN, USA

(*Received* 28 *August* 2012; *revised* 13 *December* 2012; *in final form* 12 *February* 2013)

Abstract—Up until about two decades ago acoustic imaging and ultrasound imaging were synonymous. The term *ultrasonography*, or its abbreviated version *sonography*, meant an imaging modality based on the use of ultrasonic compressional bulk waves. Beginning in the 1990s, there started to emerge numerous acoustic imaging modalities based on the use of a different mode of acoustic wave: shear waves. Imaging with these waves was shown to provide very useful and very different information about the biological tissue being examined. We discuss the physical basis for the differences between these two basic modes of acoustic waves used in medical imaging and analyze the advantages associated with shear acoustic imaging. A comprehensive analysis of the range of acoustic wavelengths, velocities and frequencies that have been used in different imaging applications is presented. We discuss the potential for future shear wave imaging applications. (E-mail: urban.matthew@mayo.edu) © **2013 World Federation for Ultrasound in Medicine & Biology.**

Key Words: **Compressional wave, Shear wave, Elasticity, Viscoelasticity, Acoustic imaging, Dispersion, Anisotropy.**

INTRODUCTION

Two decades ago, in the field of medical imaging, the terms *acoustic imaging* and *ultrasonic imaging* were synonymous. The only acoustic waves used for imaging biological structures were ultrasonic compressional (or longitudinal) waves. In the 1990s, a new acoustic imaging technology started to emerge that was based on shear (or transverse) acoustic waves. In the remainder of this article, we use the term *shear wave* to denote the entire family of transverse waves.

The wave speeds of these different kinds of waves are governed by two different types of moduli. Compressional wave speed is related to the bulk modulus of the tissue, whereas shear wave speed is related to the shear modulus. Compressional wave speed does not vary significantly for biological tissues compared with the variation of the shear wave velocity in the same tissues. For this reason, elasticity imaging, which is targeted at imaging the shear modulus of tissue, has a wide dynamic range that can be exploited (Sarvazyan et al. 1998).

The purpose of this article is to explore the differences between imaging with compressional and shear waves. We explore the ranges of relevant frequencies used in each modality and the ranges of acoustic wave speeds. We explore how different imaging techniques exploit parameters obtained with the use of shear waves and discuss regions of these parameter spaces that have yet to be explored.

Address correspondence to: Matthew W. Urban, Mayo Clinic College of Medicine, Department of Physiology and Biomedical Engineering, Rochester, MN 55905, USA. E-mail: urban.matthew@mayo.edu

MECHANISMS OF CONTRAST IN ACOUSTIC IMAGING

The wave motion in a medium is governed by the wave equation. For simplicity we assume a linear, elastic, isotropic and homogeneous medium (Manduca et al. 2001)

$$\rho \frac{\partial^2}{\partial t^2} u(\mathbf{x},t) = (\lambda+\mu)\nabla(\nabla\cdot u(x,t)) + \mu\nabla u(\mathbf{x},t), \qquad (1)$$

where ρ = mass density; λ_L and μ_L = Lamé parameters; t = time; and $\mathbf{x}$ = spatial vector defined as $\mathbf{x} = [x, y, z]$. A solution of the wave equation is given by

$$u(\mathbf{x},t) = u_0 e^{i(\omega t - k\mathbf{x})}, \qquad (2)$$

where u_0 = displacement amplitude; ω = angular frequency; and k = wavenumber: $k = \omega/c$, where c is the speed of the acoustic wave. As stated above, compressional waves have been used for more than 60 years to

image the internal structures of the body. Conventional B-mode imaging is based on differences in acoustic impedance of tissue, Z, which is given by

$$Z = \rho c_c, \tag{3}$$

where c_c = compressional wave velocity. Compressional wave velocity is related to both Lamé parameters by

$$c_c = \sqrt{\frac{\lambda_L + 2\mu_L}{\rho}} = \sqrt{\frac{E(1-v)}{\rho(1+v)(1-2v)}}. \tag{4}$$

The above relationship can also be written in terms of the bulk modulus, K, and the shear modulus, μ, where $K = \lambda_L + 2\mu_L/3$ and $\mu = \mu_L$.

$$c_c = \sqrt{\frac{K + 4\mu/3}{\rho}}. \tag{5}$$

It is shown later that the bulk modulus is typically several orders of magnitude larger than the shear modulus in tissues, so the compressional wave velocity is almost solely determined by the bulk modulus of the tissue. The bulk and shear moduli can also be written as (Sarvazyan et al. 2011)

$$K = \frac{E}{(1+v)(1-2v)}, \tag{6}$$

$$\mu = \frac{E}{2(1+v)}, \tag{7}$$

where E = compressional Young's modulus, assuming a Hookean elastic solid; and v = Poisson's ratio. In most soft tissues, Poisson's ratio is assumed to be very close to 0.5, which is the condition for incompressibility.

Both fundamental components of bulk acoustic impedance of a material, density and bulk modulus, are dependent on the molecular composition of that material. Water is the main molecular component of soft tissue; thus, the speed of compressional waves in all soft tissues lies within the range ±10% that of water (Duck 1990; Goss et al. 1978, 1980; Sarvazyan and Hill 2004). It is well known that the speed and attenuation of compressional waves in soft tissue are defined mainly by its molecular content rather than structure: disintegration, that is, mechanical homogenization of tissue, generally does not lead to substantial, immediate change in these acoustical parameters (Pauly and Schwan 1971; Sarvazyan et al. 1987). The speed of compressional waves in liver tissue samples of different levels of structural integrity (intact, ground and highly homogenized) differs less that 0.5% (Sarvazyan et al. 1987). The wave speed in the ground tissue is slightly higher than that in the intact tissue, and this small increase is explained by an increase in the level of hydration of some biopolymers released in the ground tissue. Both compressibility and density, which define compressional wave speed in tissue, are determined by short-range intermolecular interactions, and water, as the major component of soft tissue, contributes the most to these bulk properties of tissue. Therefore, the images obtained using compressional waves represent mainly the pattern of water hydrating the molecules composing the tissue (Sarvazyan and Hill 2004). This pertains to imaging of most soft tissues such as liver, kidney, heart and skeletal muscle, which contain 70%–75% water and which are the main target of ultrasonic imaging, but this is not the case for tissues like lung, cartilage and fat, which do not have a high water content.

This strong association of acoustic tissue properties with those of water becomes evident from the comparison of temperature dependences of compressional wave speed in pure water and soft tissues. The most characteristic acoustical feature of water is a unique non-linear temperature dependence of sound speed resulting from the temperature-induced changes in the dynamics of hydrogen-bonded clusters. No other fluid or substance has similar dependence. The temperature dependence of compressional wave speed in tissue closely resembles that of pure water (Fig. 1) (Sarvazyan et al. 2005).

Although conventional sonography is based mainly on visualizing the spatial distribution of acoustic impedance, which is defined by short-range molecular interactions in the tissue, the imaging based on the use of shear waves shows quite a different set of macroscopic structural features determined by long-range molecular and cellular interactions (Sarvazyan 2001; Sarvazyan and Hill 2004).

Shear waves have been used over the last two decades to explore the underlying material properties of soft tissues (Sarvazyan et al. 2011). Shear wave speed is dependent on the shear modulus of the material as given by

$$c_s = \sqrt{\frac{\mu}{\rho}} = \sqrt{\frac{E}{2\rho(1+v)}}. \tag{8}$$

The shear modulus of a material is highly dependent on tissue architecture and structural makeup. This tissue architecture varies greatly depending on the organ and its state. For example, the liver is largely isotropic and homogenous with an intricate series of blood vessels running through it so that the liver can filter the blood supply. Alternatively, other organs are very specifically arranged. Skeletal muscle can be assumed to be transversely anisotropic. That is, it is arranged into bundles of fibers in a semi-crystalline architecture. In this case,

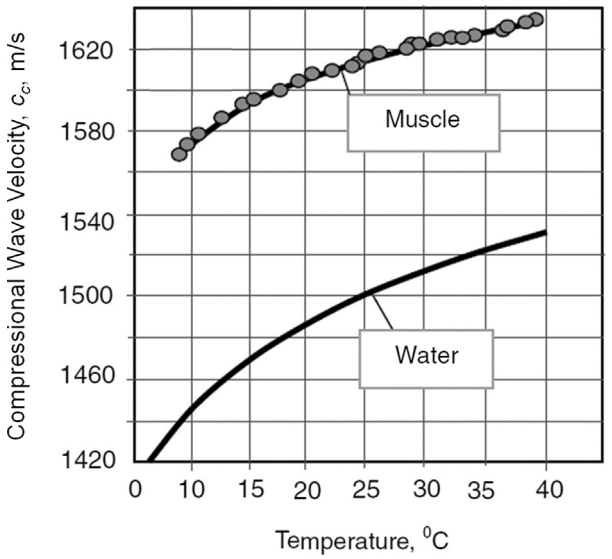

Fig. 1. Variation of compressional phase velocity in skeletal muscle and pure water. © 2004 Elsevier. Reproduced with permission from Sarvazyan et al. (2005).

there are different values of the shear modulus along the muscle fibers and perpendicular to the muscle fiber direction (Chen et al. 2009; Gennisson et al. 2003, 2010; Lee et al. 2012a; Urban and Greenleaf 2009). Lee et al. (2012a) measured the moduli in a material with orthotropic symmetry. The shear modulus tensor can be written as

$$M = \begin{bmatrix} \mu_{11} & \mu_{12} \\ \mu_{12} & \mu_{22} \end{bmatrix} = R \begin{bmatrix} \mu_{//} & 0 \\ 0 & \mu_{\perp} \end{bmatrix} R^T, \tag{9}$$

where

$$R = \begin{bmatrix} \cos(\theta) & -\sin(\theta) \\ \sin(\theta) & \cos(\theta) \end{bmatrix} \tag{10}$$

$\mu_{//}$ and $\mu_{\perp}$ = shear moduli parallel and perpendicular to the muscle fibers; and θ = angle with respect to the muscle fiber longitudinal direction. Each of the moduli can be calculated using eqn (8). The value of $\mu_{//}$ is assumed to be the largest eigenvalue found in the material.

Other organs such as the heart and skin consist of different layers. In the case of the heart wall, the layers are oriented at different angles through the thickness (Couade et al. 2011; Lee et al. 2012b; Sosnovik et al. 2001). The dependence of shear wave behavior on these different long-range molecular and cellular characteristics has provided the opportunity to investigate some new and fundamental tissue propertie with ultrasound methods.

In contrast to compressional waves, shear waves are polarized, which makes them sensitive to tissue anisotropy, an important structural anatomic characteristic that can have diagnostic value. This is illustrated by the shear wave displacements in Figure 2 in the axial and radial directions, in which the distributions are very different in two orthogonal directions. Therefore, by directing shear waves in different directions, it could be possible to characterize tissue anisotropy.

There are two other aspects that can cause variation in shear wave velocities. Up until now, we have assumed that soft tissues behave as elastic materials. However, many studies have reported that biological tissues are more appropriately characterized as viscoelastic materials; that is, their deformation depends on the time course of the stress applied. To incorporate this viscoelasticity, we can define the wavenumber for the shear wave as a complex quantity

$$k = k_r + ik_i, \tag{11}$$

where $k_r = \omega/c_s$ and $k_i = \alpha_s$. Shear modulus can alternatively be defined as

$$\mu = \rho \frac{\omega^2}{k^2}. \tag{12}$$

Because k is a complex quantity, the shear modulus also becomes a complex quantity, $\mu = \mu_1 + i\mu_2$ where μ_1 = elastic or storage modulus and μ_2 = viscous or loss modulus (Vappou et al. 2009).

$$\mu_1 = \rho\omega^2 \frac{k_r^2 - k_i^2}{\left(k_r^2 + k_i^2\right)^2}, \tag{13}$$

$$\mu_2 = -2\rho\omega^2 \frac{k_r k_i}{\left(k_r^2 + k_i^2\right)^2}. \tag{14}$$

The relationships for shear wave speed and attenuation can be written as

$$c_s(\omega) = \sqrt{\frac{2\left(\mu_1^2 + \mu_2^2\right)}{\rho\left(\mu_1 + \sqrt{\mu_1^2 + \mu_2^2}\right)}}, \tag{15}$$

$$\alpha_s(\omega) = \sqrt{\frac{\rho\omega^2\left(\sqrt{\mu_1^2 + \mu_2^2} - \mu_1\right)}{2\left(\mu_1^2 + \mu_2^2\right)}}. \tag{16}$$

It is readily evident that because of the viscoelasticity of the tissue, the shear wave speed will vary with frequency, a characteristic called *dispersion*. This becomes important in the quantitative characterization of soft tissue because the frequency must be known to provide an accurate result.

The second parameter that can affect shear wave speed is the dimensions of the boundaries of the tissue

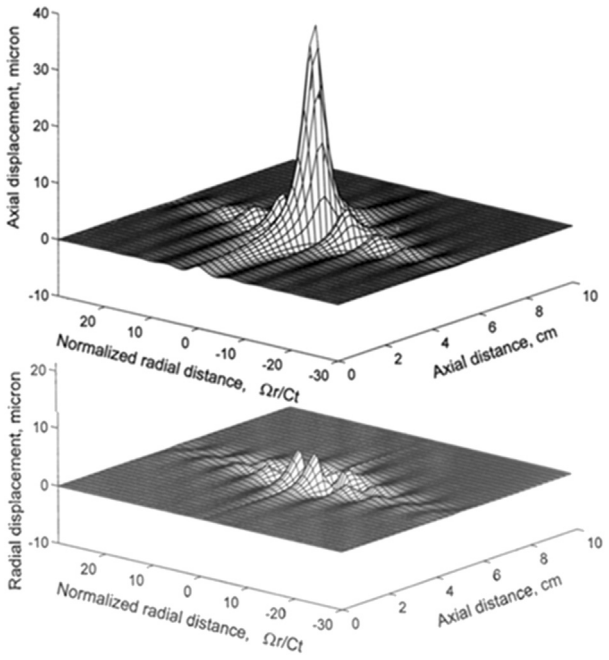

Fig. 2. Shear wave amplitude distributions in the axial and radial directions. © 1998 Elsevier. Partially reproduced with permission from Sarvazyan et al. (1998).

with respect to the wavelength being used. In this case, where the shear wavelengths are larger than the object, geometric dispersion can result even when the material is elastic. In tissues such as the heart wall, arterial wall and skin, various modes of guided waves can be generated when the thickness of these tissues is comparable to the shear wavelength. The guided wave speed is a function of both the geometry and the material properties of the tissue. One example in *ex vivo* arteries revealed multiple modes of vibration and guided wave speeds ranging from 5 to 30 m/s (Bernal et al. 2011). Lamb waves occur in plates that have been used to model the heart wall and cornea. Circumferential and flexural waves occur in cylindrical structures such as the arteries. Surface waves have been employed in the study of skin and lung.

Because the structure and constituents can vary so widely among different soft tissues, shear wave speed in soft tissues can vary over two orders of magnitude. This variation in shear wave speed increases in many tissues in the presence of disease. It is well documented that cancerous tissues can be significantly stiffer than normal tissue, particularly in tissues affected by breast and prostate cancer (Hoyt et al. 2008; Kemper et al. 2004; Krouskop et al. 1998; Lorenzen et al. 2002; Rubens et al. 1995; Sinkus et al. 2005a; Tanter et al. 2008). Additionally, disease processes that damage tissue can cause fibrotic replacement of normal tissue in organs like the liver and kidney, which, in turn, increases the stiffness and, thus, the shear wave speed of the organ (Arndt et al. 2010; Rouviere et al. 2006; Sandrin et al. 2003).

Compressional wave speed will also typically increase in these cases but the percent change is much smaller than that for shear wave speed. Diagnostic information can be obtained from the large variations in shear wave speed caused by disease (Rouviere et al. 2006; Sandrin et al. 2003; Tanter et al. 2008). Table 1 lists ranges of compressional and shear wave speeds for different types of normal and pathologic tissues.

EXAMINATION OF WAVE PARAMETERS IN ACOUSTIC IMAGING

To explore where compressional and shear waves can be used for tissue property analysis, it is useful to examine the parameter space governed by the simple equation

$$c = f\lambda, \tag{17}$$

where c = wave speed; f = frequency of the wave; and λ = wavelength. Figure 3 is a logarithmic plot of acoustic wave velocity versus frequency. Four diagonal lines are also drawn that correspond to acoustic wavelengths of 0.1, 1.0, 10.0 and 100 mm. The ability to image a material depends on the wavelength used and the characteristic dimensions of the material. To support wave propagation, the dimensions of the tissue should be larger than the wavelength, and to resolve a specific feature, the wavelength must be shorter than the dimension of that feature. Therefore, the region corresponding to large wavelengths ($\lambda > 100$ mm), is defined in Figure 3 as a "non-wave" region. Second, when the wavelength falls below 0.1 mm, wave attenuation is very high, which limits the distance these waves can travel. The desired propagation distance should be comparable to the dimensions of the structures that need to be imaged. On the basis of data on attenuation of acoustic waves in biological tissue, it can be estimated that the wavelength cannot be shorter than a few tens of microns, and the corresponding region in Figure 3 is defined as "too high attenuation." Two regions on the vertical axis, corresponding to compressional and shear wave speeds in biological tissues, are highlighted in blue. The region for compressional wave speeds ranges from 1500 to 1800 m/s and covers the frequency range $10^{5.7}$ to 10^{8} Hz. The region for shear wave velocities ranges from 0.5 to 100 m/s, and the frequencies vary from 10^{0} to 10^{6} Hz.

The first observation from Figure 3 is that the ranges of parameters related to shear waves are larger than those for compressional waves, which again highlights the increased potential for using shear waves to characterize biological tissues. Another advantage is that the shear waves extend to such low frequencies (a few hertz to

Table 1. Variation of compressional and shear wave speeds in different tissues

	Compressional waves		Shear waves	
Tissue	c_c (m/s)	References	c_s (m/s)	References
Breast	1450–1570	Duck 1990; Goss et al. 1978	1.10–3.46	Athanasiou et al. 2010; Bai et al. 2012; Lorenzen et al. 2003; Sinkus et al. 2005b, 2007; Tanter et al. 2008
Breast cancer	1437–1584	Duck 1990; Goss et al. 1978	3.25–9.64	Athanasiou et al. 2010; Bai et al. 2012; Berg et al. 2012; Evans et al. 2010; McKnight et al. 2002; Sinkus et al. 2005b, 2007; Tanter et al. 2008
Liver	1522–1623	Duck 1990; Goss et al. 1978, 1980	0.85–3.01	Asbach et al. 2010; Bavu et al. 2011; Friedrich-Rust et al. 2009; Muller et al. 2009; Rouviere et al. 2006; Palmeri et al. 2008
Fibrotic/cirrhotic liver	1535–1581	Duck 1990	0.84–5.00	Asbach et al. 2010; Bavu et al. 2011;; Castéra et al. 2010; Friedrich-Rust et al. 2009; Huwart et al. 2006; Muller et al. 2009; Sandrin et al. 2003; Stebbing et al. 2010
Skeletal muscle	1500–1610	Goss et al. 1978	1.56–7.60	Chen et al. 2009; Gennisson et al. 2003, 2010; Klatt et al. 2010; Ringleb et al. 2007; Nordez et al. 2008; Uffmann et al. 2004; Urban and Greenleaf 2009
Kidney	1558–1562	Duck 1990	1.20–3.50	Amador et al. 2011; Arndt et al. 2010; Derieppe et al. 2012; Stock et al. 2010; Syversveen et al. 2011
Heart	1528–1602	Duck 1990; Goss et al. 1978, 1980	0.83–7.00	Bouchard et al. 2009; Couade et al. 2011; Kanai 2005; Kolipaka et al. 2010; Lee et al. 2012b; Nenadic et al. 2011a, 2011c; Pernot et al. 2011
Arteries	1559–1660	Duck 1990; Goss et al. 1978	2.83–6.09	Bernal et al. 2011; Couade et al. 2010; Luo et al. 2009, 2012; Vappou et al. 2010; Zhang et al. 2005
Brain	1460–1580	Duck 1990; Goss et al. 1978, 1980	1.02–4.63	Green et al. 2008; Kruse et al. 2008; Mace et al. 2011; Sack et al. 2008, 2009; Zhang et al. 2011a
Skin	1498–1540	Goss et al. 1978	2.66–5.99	Zhang et al. 2011b
Lung	577–1472	Duck 1990; Goss et al. 1978	0.90–3.54	Goss et al. 2006; Mariappan et al. 2011, 2012; McGee et al. 2009; Zhang et al. 2011c
Spleen	1515–1635	Duck 1990; Goss et al. 1978, 1980	1.10–2.36	Mannelli et al. 2010; Nedredal et al. 2011; Nenadic et al. 2011a; Talwalkar et al. 2009
Cornea	1542–1639	Duck 1990; Goss et al. 1978, 1980	1.43–6.80	Litwiller et al. 2010; Tanter et al. 2009
Cervix/uterus	1625–1633	Duck 1990; Goss et al. 1978	2.01–2.58	Stewart et al. 2011
Thrombus	1586–1597	Duck 1990	0.33–1.27	Gennisson et al. 2006
Tendons	1631–3530	Duck 1990; Goss et al. 1978	79.4	Song 2010
Cartilage	1520–1665	Goss et al. 1978; Ling et al. 2007; Nieminen et al. 2007	39.71–87.83	Lopez et al. 2007, 2008
Bone	1630–4170	Duck 1990; Goss et al. 1978, 1980	1420–3541	Goss et al. 1978

tens of hertz for certain modes of guided waves) which cover characteristic time scales for observing certain structural and functional processes in biological tissues.

ACOUSTIC WAVE IMAGING METHODS

Having defined the parameter space in Figure 3, it is important that we examine how different investigators have explored this space with different acoustic imaging methods. This analysis also defines which regions have not been investigated to date. We discuss the potential of future applications related to those heretofore unexplored regions.

Imaging with compressional waves

Within the region defined by the compressional waves, B-mode ultrasound imaging is typically performed using frequencies ranging from 1 to 15 MHz. Echocardiography and abdominal imaging typically are performed at lower frequencies ranging from 1 to 4 MHz. These lower frequencies are used because the structures of interest are typically 4 to 15 cm deep, and the attenuation at these frequencies is lower. For more superficial applications such as imaging of the breast, thyroid and vasculature, higher ultrasound frequencies ranging from 5 to 15 MHz are used. These higher frequencies provide higher spatial resolution,

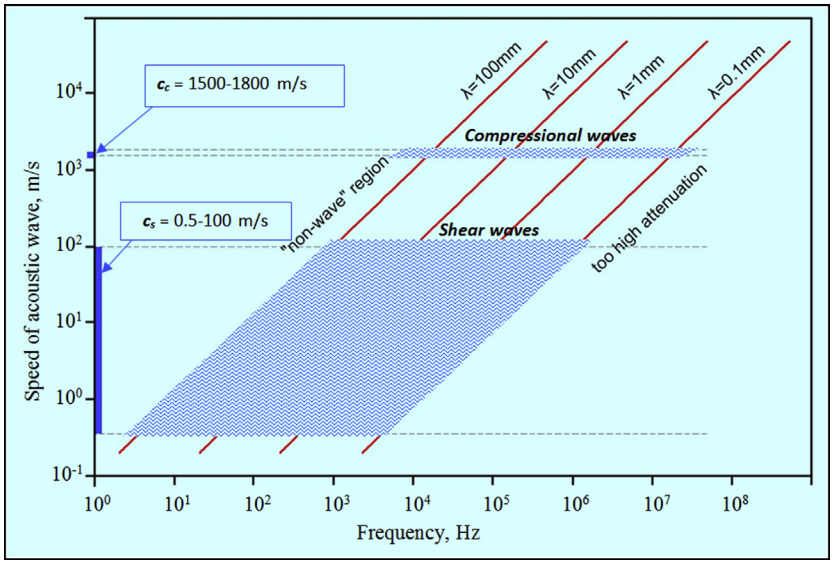

Fig. 3. Acoustic imaging feature space. The ranges of compressional and shear wave speeds are given by c_c and c_s.

which is typically needed to resolve small structural details. For ophthalmic applications, high frequencies ranging from 10 to 20 MHz are used. It is important to note that there are no appreciable gaps in frequency for using compressional waves for diagnostic acoustic imaging.

Imaging with shear waves

A number of methods have been developed to generate and measure the propagation of shear waves in tissue. These techniques are often defined by how they excite the shear wave as well as how they are measured. A recent review provides a comprehensive overview of these different methods and the types of applications in which they have been used (Sarvazyan et al. 2011). We briefly describe those methods and the frequencies typically used. The frequencies used are typically determined by the application.

One of the early methods used to generate propagating shear waves in tissue was external mechanical actuation. Krouskop et al. (1987) used a mechanical actuator on the quadriceps muscle while measuring the motion with Doppler ultrasound. Similar measurements were soon reported by Yamakoshi et al. (1990), who made measurements in human liver. Additionally, a method called *sonoelasticity imaging* was reported that used vibration to examine soft tissue (Lerner et al. 1990; Parker et al. 1990). The vibration was measured using Doppler ultrasound methods, and the wave motion was analyzed using a model based on a Bessel function expansion of the Doppler signals. About a decade after these developments, a related method called *sonoelastography imaging* was developed that used two mechanical drivers exciting the tissue at slightly different frequencies to create "crawling waves" at the beat frequency of the two drivers (Wu et al. 2004).

Another method that used mechanical actuation is called *magnetic resonance elastography* (MRE). The resulting shear waves were measured with magnetic resonance imaging (MRI) techniques (Muthupillai et al. 1995). This technique uses harmonic waves at a specific frequency typically ranging from 20 to 200 Hz, although some applications have been performed at frequencies ranging from 500 to 9000 Hz (Kruse et al. 2000; Lopez et al. 2007, 2008; Manduca et al. 2001). Recently, MRE measurements on a viscoelastic silicone rubber over a large bandwidth, 200–7750 Hz, were reported (Yasar et al. 2012). One of the unique elements of this study is that three different sample sizes were used in two different MR scanners, and the overlap between these samples and scanners was quite good. MRE applications have been reviewed thoroughly by several authors (Mariappan et al. 2010; Litwiller et al. 2012; Sinkus et al. 2012).

Transient elastography (TE) is a method that was developed to measure the transient shear waves produced by an impulsive mechanical actuation (Sandrin et al. 2002a, 2002b). This method was used to make measurements in various types of tissues, but has found widespread use in measuring liver stiffness after being commercialized by EchoSens (Paris, France) as a product called FibroScan. In the liver application, the frequency used is typically 50 Hz (Sandrin et al. 2003).

In the mid-1990s, another method was introduced to create shear waves that involved the use of focused ultrasound to produce acoustic radiation force. This approach was derived from studies that started to use ultrasound radiation force to perturb tissue. Sugimoto et al. (1990)

were among the first to use radiation force to investigate tissue hardness. Subsequent developments of methods called *vibro–acoustography* by Fatemi and Greenleaf (1998, 1999) and *acoustic radiation force impulse imaging* by Nightingale et al. (2001) also used radiation force to stimulate tissue and measure the mechanical response. These contributions served as motivation for later developments in the use of radiation force to generate shear waves (Nightingale et al. 2003; Sarvazyan et al. 1998).

Chen et al. (2004) used modulated ultrasound to produce harmonic radiation force at frequencies ranging from 100 to 500 Hz. This harmonic radiation force produced shear waves at known frequencies, and the shear waves were measured using a laser vibrometer in gelatin phantoms. These measurements were used to characterize the viscoelastic properties of the phantoms.

Other groups used tone bursts of ultrasound. The length of the pulses used for creating the radiation force typically ranges from 50 to 1000 μs. For these types of pulses, the tissue reacts as if the excitation is impulsive, so many frequencies can be excited at the same time. Multiple methods have been developed using this impulsive radiation force coupled with ultrasound imaging techniques to measure the propagating shear waves. These methods include shear wave elasticity imaging (Nightingale et al. 2003; Palmeri et al. 2008; Sarvazyan et al. 1998), supersonic shear imaging (SSI) (Bercoff et al. 2004; Fink and Tanter 2011), shear wave dispersion ultrasound vibrometry (SDUV) (Chen et al. 2004, 2009; Urban et al. 2012), spatially modulated ultrasound radiation force (SMURF) (McAleavey et al. 2007) and sonoelastography using radiation force (Hah et al. 2012; Hazard et al. 2012). These various methods have been applied to many types of tissues. Two radiation force–based methods, SSI and SWEI, have been commercialized for clinical use on the SuperSonic Imagine Aixplorer as Shear Wave Elastography and on the Siemens Acuson S2000 as Virtual Touch Quantification. The frequencies used in these methods typically range from 50 to 1000 Hz, and the shear wave velocities, from 0.5 to 12 m/s.

Investigation of certain tissues such as the heart, arteries and cornea with acoustic radiation force produces guided waves (Bernal et al. 2011; Brum et al. 2012; Couade et al. 2010; Kanai 2005; Nenadic et al. 2011a, 2011b, 2011c; Tanter et al. 2009). These waves are strongly affected by the geometry of the organ, and wave velocities are governed by the material properties and geometric structure. Guided wave velocities can range from 1 to 30 m/s, and the frequency range is quite large, 100–7000 Hz.

A few methods have been reported that use endogenous motion of certain organs, typically associated with the beating of the heart. Kanai (2005, 2009) made measurements of the waves present in the heart as it beats. A method called *electromechanical imaging* has been used to measure the electromechanical waves propagating in the heart wall and the pulse waves propagating in arterial vasculature (Konofagou et al. 2011; Pernot et al. 2007; Provost et al. 2011; Vappou et al. 2010; Wang et al. 2008). A method that uses passive tomography methods was adapted from the field of seismology; it uses physiologic motion to measure shear wave velocity in various soft tissues (Benech et al. 2009; Gallot et al. 2011). The frequency range for these methods is quite low because typical heart rates range from 0.8 to 2.0 Hz.

Lastly, there are methods that perturb the tissue using acoustic radiation force and measure the resulting tissue deformation directly or indirectly. One such method is called *vibro-acoustography,* in which two beams of ultrasound with slightly different frequencies are used to create acoustic radiation force at the difference frequency, Δf, between the two beams (Fatemi and Greenleaf 1998, 1999; Urban et al. 2011). The values for Δf typically range from 40 to 120 kHz. The beating radiation force stimulates an acoustic response, resulting in a propagating compressional wave at Δf. This acoustic wave is measured by a nearby hydrophone. The excitation beam is scanned over an object to create an image. In another method called *harmonic motion imaging*, modulated ultrasound is used to create a harmonic radiation force at frequencies of 10–200 Hz (Konofagou and Hynynen 2003; Konofagou and Maleke 2011; Maleke and Konofagou 2008). The displacement of the tissue is measured with ultrasound techniques, and the excitation beam is scanned over the object to create an image.

ANALYSIS OF ACOUSTIC IMAGING FEATURE SPACE

With this background on the various methods employed to measure acoustic waves in biological tissues, we can turn to a modified version of Figure 3 in which we overlay colored sections (Fig. 4) indicating how these various methods cover the spaces occupied by the modalities that use compressional and shear waves to image tissue. Within the imaging space occupied by using compressional waves, the portion occupied by diagnostic B–mode imaging could be subdivided by frequency based on application areas.

Most shear wave applications occupy the space in the lower left corner of the speed/frequency space. Methods that use endogenous motion lie in the most extreme part of the space because of the low-frequency content present in the physiologic motion. One other low-frequency effect may be the poroelastic behavior of the tissue that occurs at frequencies much lower than

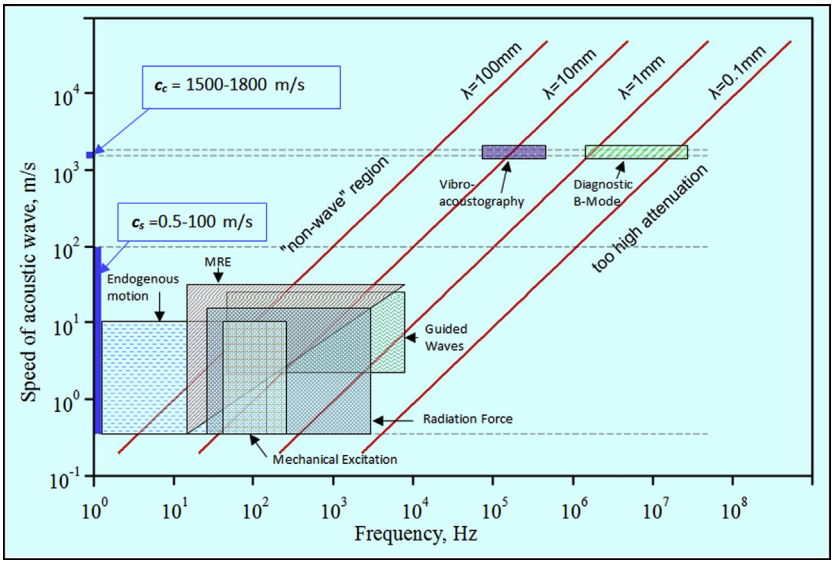

Fig. 4. Acoustic imaging feature space with regions depicting methods used for shear and compressional acoustic wave imaging.

those depicted in the feature space of Figure 3 (Berry et al. 2006a, 2006b; Konofagou et al. 2001; Righetti et al. 2004, 2005). MRE and the methods that use acoustic radiation force most often operate in the bandwidth 50–500 Hz. The methods that use mechanical excitation are more often limited to lower-frequency ranges than methods that use acoustic radiation force. In special applications that involve guided waves, particularly those that explore viscoelastic and/or geometry-based wave speed dispersion, frequencies extend to a few kilohertz.

There exists a substantial lack of data for tissues with very high shear wave speeds. These types of tissue would typically be either cancerous tissues or very fibrotic tissues. Additionally, tissues such as tendons, cartilage and cancellous and cortical bone would also have very high shear wave speeds ($c_s > 20$ m/s). In tissue engineering applications, cartilage can be grown, and as it matures, the elastic modulus increases along a continuum (Huang et al. 2010). In studies that examine the digestion of cartilage to analyze the contributions of the constituents, a wide range of elastic moduli have also been found (Stolz et al. 2004). Although there are not a lot of data in the elasticity imaging community on these types of materials, measurements could potentially be made to quantify the mechanical properties with shear or guided waves.

Measuring shear wave speed in materials with high shear wave speeds is difficult for two reasons. First, a high shear wave speed inherently implies that the tissue is stiff, so the same stress that is applied in soft tissues will produce markedly lower displacements in these stiffer tissues. The minimum motion that most ultrasound-based methods can measure is typically 0.1 μm. A second issue is that because the waves move so fast, a very high frame rate must be used to measure the shear waves. The tissue motion must be tracked at several lateral locations through time to make a reliable estimate of shear wave speed. If the number of spatial locations is limited or the measurement interval is too long, then these fast waves may not be evaluated correctly.

To analyze this problem, a theoretical treatment of shear wave phase velocity estimation was given by Urban et al. (2009). Shear wave phase velocity is the velocity at which each frequency component of the shear wave travels. The conclusions of this study were that errors can be decreased with increased shear wave displacement amplitude, increased number of lateral locations used for shear wave estimation and increased signal-to-noise ratio in received ultrasound echoes. This same theoretical framework could be adapted to examine a time domain-based time-of-flight estimation of shear wave group velocity. Shear wave group velocity is the velocity at which the wave packet travels.

These two aforementioned problems regarding displacement amplitude and increasing measurement frame rate can be addressed in a few ways. To induce more motion, the radiation force could be increased either by extending the excitation tone burst or by increasing the ultrasound intensity. Both of these approaches may be limited for clinical implementation because these methods must comply with regulatory limits on mechanical index (MI) and spatial-peak temporal average intensities (I_{spta}) set by the Food and Drug Administration (Herman and Harris 2002). As an alternative to radiation force, mechanical actuation can be used to produce more

motion. This may increase the complexity of a particular method because of inaccessibility to the organ of choice or issues relating to alignment of the actuator and measurement device.

To increase the temporal resolution of the measurement, fewer spatial locations can be measured, or a single location can be measured with M-mode ultrasound and the excitation can be repeated for every spatial measurement location to synthetically examine the wave propagation. In this case, measurements could be made with frame rates in the kilohertz range. This approach may be prohibitive for the amount of time it might take, particularly to make images. Another technique that has come into practice is to insonify the medium with a plane wave and perform beam forming only in receive (Bercoff et al. 2004). This method can be repeated at very high frame rates (up to 20,000 frames per second), but the signal-to-noise ratio is typically poor. Coherent compounding with plane wave insonifications at different angles is one way to reclaim adequate signal-to-noise ratios to make reliable shear wave velocity measurements (Montaldo et al. 2009).

Biological tissues that have higher shear wave speed also typically are thin in nature, such as cartilage and cortical bone. To make images of these materials, shorter shear wavelengths are needed, which would require higher frequencies. Waves with these higher frequencies with sufficient motion amplitude may be difficult to excite for the reasons discussed above. Using guided waves of lower frequencies may provide a solution for measuring these types of tissues, but methods have yet to be developed to address this.

Another region that has yet to be explored in detail is the "high attenuation" area where shear wavelengths are very small. This region is significant because it includes shear modulus variations at the microscopic level. It is of significant interest for researchers in this field of elasticity imaging to relate how changes in the microenvironment translate into changes in the shear modulus measured at the macroscopic level. A greater understanding of these relationships could provide scientists and clinicians with useful information for understanding various disease processes including tissue fibrosis and cancer.

SHEAR WAVE IMAGING AS A "MULTIWAVE" APPROACH

Mathias Fink and his colleagues coined the term *multiwave imaging* to describe various methods used in elasticity imaging (Fink and Tanter 2010, 2011). This description is particularly pertinent to this discussion of acoustic imaging. In almost all of the methods described, a multiwave approach is taken to generate and/or measure shear waves. When mechanical actuation is used, a pure shear actuator is rarely used. Instead, the actuator is typically inducing a compressional wave as well as a shear wave. The compressional wave typically has very low amplitude and travels very fast, so it is rarely reliably measured.

In methods that use acoustic radiation force, compressional ultrasound waves of sufficiently high intensity are used to displace the tissue and cause shear waves. Additionally, the motion detection, which is inherently necessary in all of the methods discussed, provides another circumstance of multiwave imaging. Compressional ultrasound waves are used to interrogate the tissue repeatedly to estimate the motion caused by shear wave propagation. In MRE, electromagnetic waves are used to measure the tissue deformation.

DISPERSION IN SHEAR WAVE MEASUREMENTS

Many methods use the group velocity of the shear wave to characterize the material properties of tissue. When group velocity is used, it is typically assumed that the material is elastic and that the object is much larger than the shear wavelengths. These assumptions neglect dispersion caused by either viscosity or finite geometry of the material. As a result, reporting only the group velocity could lead to bias in measurements if the effects of dispersion are neglected. It is imperative that if only group velocity is documented in studies, the frequency of the wave should also be reported so that the effects of dispersion may be assessed.

As many published reports have documented, soft tissues are inherently viscoelastic. One advantage of using shear waves for characterization of tissue is that shear wave speeds exhibit dispersion. Multiple groups have examined the dispersion of shear waves in various soft tissues (Amador et al. 2011; Asbach et al. 2008, 2010; Bernal et al. 2011; Chen et al. 2009; Couade et al. 2010; Deffieux et al. 2009; Gennisson et al. 2010; Kanai 2005; Klatt et al. 2007; Kruse et al. 2000; Mitri et al. 2011; Muller et al. 2009; Nenadic et al. 2011c; Tanter et al. 2008; Urban and Greenleaf 2009; Yamakoshi et al. 1990). Some groups use individual frequencies with mechanical actuation, whereas others use impulsive shear waves generated using acoustic radiation force. The advantage of using acoustic radiation force is that many different frequencies can be excited in one acquisition. These shear waves can have large bandwidths typically ranging from 100 to 500 Hz and, in some cases, up to 1500 Hz (Bernal et al. 2011; Couade et al. 2010). With larger bandwidths, the dispersion of shear wave velocities can be more fully characterized and used to evaluate the elastic and viscous components of the tissue. Viscosity has been evaluated

in a few different studies, but requires more exploration in different tissues to assess its usefulness as a biomarker of tissue health (Chen et al. 2009; Huwart et al. 2006). The large frequency range of the shear wave velocity feature space provides potential for using high-bandwidth shear waves for viscoelastic property estimation.

Dispersion has also been used in the context of guided waves in tissues with specific geometries, particularly the heart, arteries and cornea (Bernal et al. 2011; Couade et al. 2010; Brum et al. 2012; Kanai 2005; Nenadic et al. 2011a, 2011b, 2011c; Tanter et al. 2009). As mentioned above, the dispersion in the measured wave velocities arises because of tissue viscoelasticity and geometry. Through the use of acoustic radiation force, waves with large bandwidths can be generated that can induce different modes of vibration within the tissue structure. Specific modes of vibration can be used in conjunction with geometric measurements and a model to sensitively assess the viscoelastic properties of the tissue (Bernal et al. 2011; Nenadic et al. 2011c).

POTENTIAL DIRECTIONS OF FUTURE RESEARCH USING SHEAR WAVES

As discussed, there remains a broad region of shear wave feature space that has yet to be explored, particularly for tissues with high shear wave velocities at the upper end of the frequency range.

One notable feature of shear waves is that they are polarized, allowing their use in the study of tissue anisotropy Compressional waves are polarized as well, but if we revisit eqn (5), the compressional modulus and density do not change with direction, so the polarization is due only to the shear modulus. For example, compressional wave speeds in sheletal muscle were shown to change as a function of fiber orientation and contraction state, but the change was at most 0.6% (Mol and Breddels 1982). Previously reported studies have taken advantage of this feature to explore the anisotropy present in skeletal and cardiac muscle (Chen et al. 2009; Gennisson et al. 2003, 2010; Lee et al. 2012b; Urban and Greenleaf 2009). Another organ that has also been examined in terms of its anisotropy is the kidney. The kidney consists of a network of tubules that are oriented radially. As a result, shear wave measurements made along or perpendicular to this radial orientation produce different results (Amador et al. 2011).

Another area that has only been studied in a preliminary fashion is elastic non-linearity of soft solids. Nonlinear properties of tissue, as they relate to elasticity, have not been adequately addressed and may provide another parameter that could serve as a clinically relevant indicator (Catheline et al. 2003; Gennisson et al. 2007; Latorre-Ossa et al. 2012).

CONCLUSIONS

Shear acoustic imaging has been developed into a clinical imaging modality over the last two decades. Comparisons and contrasts between imaging with compressional and shear waves were described. Shear wave speeds are sensitive to tissue structure, such as anisotropy. Shear material properties have a large dynamic range, which provides large potential for characterizing different types of tissue, normal or pathologic. Additionally, there is a large frequency range over which shear wave measurements can be made, providing possibilities to evaluate soft tissue shear wave speed dispersion. This dispersion, whether caused by viscoelasticity or geometry or a combination of these two factors, can be used to sensitively evaluate material properties of the studied tissue. Some of the regions of the range of shear wave phase velocities have been studied by currently available methods, but there are some regions in this frequency/phase velocity space that have yet to be exploited. Also, parameters such as tissue anisotropy, viscosity and non-linearity can be characterized using shear waves. These parameters may serve as interesting biomarkers that could yield important diagnostic information. Shear acoustic imaging is still a young imaging modality that will continue to develop and has substantial potential for characterizing different soft tissues for clinical diagnosis.

Acknowledgments—This work was supported in part by Grants EB002640, EB002167 and DK082408 from the National Institute of Biomedical Imaging and Bioengineering and National Institute of Diabetes and Digestive and Kidney Diseases. The content is solely the responsibility of the authors and does not necessarily represent the official views of the National Institute of Biomedical Imaging and Bioengineering, National Institute of Diabetes and Digestive and Kidney Diseases or the National Institutes of Health.

REFERENCES

Amador C, Urban MW, Chen S, Greenleaf JF. Shearwave dispersion ultrasound vibrometry (SDUV) on swine kidney. IEEE Trans Ultrason Ferroelectr Freq Control 2011;58:2608–2619.

Arndt R, Schmidt S, Loddenkemper C, Grünbaum M, Zidek W, Van Der Giet M, Westhoff TH. Noninvasive evaluation of renal allograft fibrosis by transient elastography: A pilot study. Transplant Int 2010;23:871–877.

Asbach P, Klatt D, Hamhaber U, Braun J, Somasundaram R, Hamm B, Sack I. Assessment of liver viscoelasticity using multifrequency MR elastography. Magn Reson Med 2008;60:373–379.

Asbach P, Klatt D, Schlosser B, Biermer M, Muche M, Rieger A, Loddenkemper C, Somasundaram R, Berg T, Hamm B, Braun J, Sack I. Viscoelasticity-based staging of hepatic fibrosis with multifrequency MR elastography. Radiology 2010;257:80–86.

Athanasiou A, Tardivon A, Tanter Ml, Sigal-Zafrani B, Bercoff J, Deffieux T, Gennisson JL, Fink M, Neuenschwander S. Breast lesions: Quantitative elastography with supersonic shear imaging: Preliminary results. Radiology 2010;256:297–303.

Bai M, Du L, Gu J, Li F, Jia X. Virtual touch tissue quantification using acoustic radiation force impulse technology. J Ultrasound Med 2012;31:289–294.

Bavu É, Gennisson J-L, Couade M, Bercoff J, Mallet V, Fink M, Badel A, Vallet-Pichard A, Nalpas B, Tanter M, Pol S. Noninvasive in vivo liver fibrosis evaluation using supersonic shear imaging: A clinical study on 113 hepatitis C virus patients. Ultrasound Med Biol 2011;37:1361–1373.

Benech N, Catheline S, Brum J, Gallot T, Negreira C. 1-D elasticity assessment in soft solids from shear wave correlation: The time-reversal approach. IEEE Trans Ultrasonics Ferroelectr Freq Control 2009;56:2400–2410.

Bercoff J, Tanter M, Fink M. Supersonic shear imaging: A new technique for soft tissue elasticity mapping. IEEE Trans Ultrason Ferroelectr Freq Control 2004;51:396–409.

Berg WA, Cosgrove DO, Doré CJ, Schäfer FKW, Svensson WE, Hooley RJ, Ohlinger R, Mendelson EB, Balu-Maestro C, Locatelli M, Tourasse C, Cavanaugh BC, Juhan V, Stavros AT, Tardivon A, Gay J, Henry J-P, Cohen-Bacrie C. Shear-wave elastography improves the specificity of breast US: The BE1 multinational study of 939 masses. Radiology 2012;262:435–449.

Bernal M, Nenadic I, Urban MW, Greenleaf JF. Material property estimation for tubes and arteries using ultrasound radiation force and analysis of propagating modes. J Acoust Soc Am 2011;129: 1344–1354.

Berry GP, Bamber JC, Armstrong CG, Miller NR, Barbone PE. Towards an acoustic model-based poroelastic imaging method: I. Theoretical foundation. Ultrasound Med Biol 2006a;32:547–567.

Berry GP, Bamber JC, Miller NR, Barbone PE, Bush NL, Armstrong CG. Towards an acoustic model-based poroelastic imaging method: II. Experimental investigation. Ultrasound Med Biol 2006b;32:1869–1885.

Bouchard RR, Hsu SJ, Wolf PD, Trahey GE. In vivo cardiac, acoustic-radiation-force-driven, shear wave velocimetry. Ultrasonic Imaging 2009;31:201–213.

Brum J, Gennisson JL, Thu-Mai N, Benech N, Fink M, Tanter M, Negreira C. Application of 1-D transient elastography for the shear modulus assessment of thin-layered soft tissue: Comparison with supersonic shear imaging technique. IEEE Trans Ultrasonics Ferroelectr Freq Control 2012;59:703–714.

Castéra L, Foucher J, Bernard P-H, Carvalho F, Allaix D, Merrouche W, Couzigou P, de Lédinghen V. Pitfalls of liver stiffness measurement: A 5-year prospective study of 13,369 examinations. Hepatology 2010;51:828–835.

Catheline S, Gennisson JL, Fink M. Measurement of elastic nonlinearity of soft solid with transient elastography. J Acoust Soc Am 2003;114: 3087–3091.

Chen S, Fatemi M, Greenleaf JF. Quantifying elasticity and viscosity from measurement of shear wave speed dispersion. J Acoust Soc Am 2004;115:2781–2785.

Chen S, Urban MW, Pislaru C, Kinnick R, Zheng Y, Yao A, Greenleaf JF. Shearwave dispersion ultrasound vibrometry (SDUV) for measuring tissue elasticity and viscosity. IEEE Trans Ultrason Ferroelectr Freq Control 2009;56:55–62.

Couade M, Pernot M, Messas E, Bel A, Ba M, Hagège A, Fink M, Tanter M. In vivo quantitative mapping of myocardial stiffening and transmural anisotropy during the cardiac cycle. IEEE Trans Med Imaging 2011;30:295–305.

Couade M, Pernot M, Prada C, Messas E, Emmerich J, Bruneval P, Criton A, Fink M, Tanter M. Quantitative assessment of arterial wall biomechanical properties using shear wave imaging. Ultrasound Med Biol 2010;36:1662–1676.

Deffieux T, Montaldo G, Tanter M, Fink M. Shear wave spectroscopy for in vivo quantification of human soft tissues visco-elasticity. IEEE Trans Med Imaging 2009;28:313–322.

Derieppe M, Delmas Y, Gennisson J-L, Deminière C, Placier S, Tanter M, Combe C, Grenier N. Detection of intrarenal microstructural changes with supersonic shear wave elastography in rats. Eur Radiol 2012;22:243–250.

Duck FA. Physical properties of tissue. London: Academic Press; 1990.

Evans A, Whelehan P, Thomson K, McLean D, Brauer K, Purdie C, Jordan L, Baker L, Thompson A. Quantitative shear wave ultrasound elastography: Initial experience in solid breast masses. Breast Cancer Res 2010;12:R104.

Fatemi M, Greenleaf JF. Ultrasound-stimulated vibro-acoustic spectrography. Science 1998;280:82–85.

Fatemi M, Greenleaf JF. Vibro-acoustography: An imaging modality based on ultrasound-stimulated acoustic emission. Proc Natl Acad Sci USA 1999;96:6603–6608.

Fink M, Tanter M. Multiwave imaging and super resolution. Phys Today 2010;63:28–33.

Fink M, Tanter M. A multiwave imaging approach for elastography. Curr Med Imaging Rev 2011;7:340–349.

Friedrich-Rust M, Wunder K, Kriener S, Sotoudeh F, Richter S, Bojunga J, Herrmann E, Poynard T, Dietrich CF, Vermehren J, Zeuzem S, Sarrazin C. Liver fibrosis in viral hepatitis: Noninvasive assessment with acoustic radiation force impulse imaging versus transient elastography. Radiology 2009;252:595–604.

Gallot T, Catheline S, Roux P, Brum J, Benech N, Negreira C. Passive elastography: Shear-wave tomography from physiological-noise correlation in soft tissues. IEEE Trans Ultrasonics Ferroelectr Freq Control 2011;58:1122–1126.

Gennisson J-L, Deffieux T, Macé E, Montaldo G, Fink M, Tanter M. Viscoelastic and anisotropic mechanical properties of in vivo muscle tissue assessed by supersonic shear imaging. Ultrasound Med Biol 2010;36:789–801.

Gennisson JL, Catheline S, Chaffai S, Fink M. Transient elastography in anisotropic medium: Application to the measurement of slow and fast shear wave speeds in muscles. J Acoust Soc Am 2003;114: 536–541.

Gennisson JL, Lerouge S, Cloutier G. Assessment by transient elastography of the viscoelastic properties of blood during clotting. Ultrasound Med Biol 2006;32:1529–1537.

Gennisson JL, Renier M, Catheline S, Barriere C, Bercoff J, Tanter M, Fink M. Acoustoelasticity in soft solids: Assessment of the nonlinear shear modulus with the acoustic radiation force. J Acoust Soc Am 2007;122:3211–3219.

Goss BC, McGee KP, Ehman EC, Manduca A, Ehman RL. Magnetic resonance elastography of the lung: Technical feasibility. Magn Reson Med 2006;56:1060–1066.

Goss SA, Johnston RL, Dunn F. Comprehensive compilation of empirical ultrasonic properties of mammalian tissues. J Acoust Soc Am 1978;64:423–457.

Goss SA, Johnston RL, Dunn F. Compilation of empirical ultrasonic properties of mammalian tissues. II. J Acoust Soc Am 1980;68: 93–108.

Green MA, Bilston LE, Sinkus R. In vivo brain viscoelastic properties measured by magnetic resonance elastography. NMR Biomed 2008;21:755–764.

Hah Z, Hazard C, Mills B, Barry C, Rubens D, Parker K. Integration of crawling waves in an ultrasound imaging system: Part 2. Signal processing and applications. Ultrasound Med Biol 2012;38:312–323.

Hazard C, Hah Z, Rubens D, Parker K. Integration of crawling waves in an ultrasound imaging system. Part 1: System and design considerations. Ultrasound Med Biol 2012;38:296–311.

Herman BA, Harris GR. Models and regulatory considerations for transient temperature rise during diagnostic ultrasound pulses. Ultrasound Med Biol 2002;28:1217–1224.

Hoyt K, Castaneda B, Zhang M, Nigwekar P, di Sant'Agnese PA, Joseph JV, Strang J, Rubens DJ, Parker KJ. Tissue elasticity properties as biomarkers for prostate cancer. Cancer Biomarkers 2008;4: 213–225.

Huang AH, Farrell MJ, Mauck RL. Mechanics and mechanobiology of mesenchymal stem cell-based engineered cartilage. J Biomech 2010;43:128–136.

Huwart L, Peeters F, Sinkus R, Annet L, Salameh N, ter Beek LC, Horsmans Y, Van Beers BE. Liver fibrosis: Non-invasive assessment with MR elastography. NMR Biomed 2006;19:173–179.

Kanai H. Propagation of spontaneously actuated pulsive vibration in human heart wall and in vivo viscoelasticity estimation. IEEE Trans Ultrason Ferroelectr Freq Control 2005;52:1931–1942.

Kanai H. Propagation of vibration caused by electrical excitation in the normal human heart. Ultrasound Med Biol 2009;35:936–948.

Kemper J, Sinkus R, Lorenzen J, Nolte-Ernsting C, Stork A, Adam G. MR elastography of the prostate: Initial in-vivo application. Rofo 2004;176:1094–1099.

Klatt D, Hamhaber U, Asbach P, Braun J, Sack I. Noninvasive assessment of the rheological behavior of human organs using multifrequency MR elastography: A study of brain and liver viscoelasticity. Phys Med Biol 2007;52:7281–7294.

Klatt D, Papazoglou S, Braun J, Sack I. Viscoelasticity-based MR elastography of skeletal muscle. Phys Med Biol 2010;55:6445.

Kolipaka A, Araoz PA, McGee KP, Manduca A, Ehman RL. Magnetic resonance elastography as a method for the assessment of effective myocardial stiffness throughout the cardiac cycle. Magn Reson Med 2010;64:862–870.

Konofagou E, Lee W-N, Luo J, Provost J, Vappou J. Physiologic cardiovascular strain and intrinsic wave imaging. Annu Rev Biomed Eng 2011;13:477–505.

Konofagou EE, Harrigan TP, Ophir J, Krouskop TA. Poroelastography: Imaging the poroelastic properties of tissues. Ultrasound Med Biol 2001;27:1387–1397.

Konofagou EE, Hynynen K. Localized harmonic motion imaging: Theory, simulations and experiments. Ultrasound Med Biol 2003; 29:1405–1413.

Konofagou EE, Maleke C. Harmonic motion imaging (HMI) for tumor imaging and treatment monitoring: A review. Curr Med Imaging Rev 2011;8:16–26.

Krouskop TA, Dougherty DR, Vinson FS. A pulsed Doppler ultrasonic system for making noninvasive measurements of the mechanical properties of soft tissue. J Rehabil Res Dev 1987;24:1–8.

Krouskop TA, Wheeler TM, Kallel F, Garra BS, Hall T. Elastic moduli of breast and prostate tissues under compression. Ultrasonic Imaging 1998;20:260–274.

Kruse SA, Rose GH, Glaser KJ, Manduca A, Felmlee JP, Jack CR, Ehman RL. Magnetic resonance elastography of the brain. NeuroImage 2008;39:231–237.

Kruse SA, Smith JA, Lawrence AJ, Dresner MA, Manduca A, Greenleaf JF, Ehman RL. Tissue characterization using magnetic resonance elastography: Preliminary results. Phys Med Biol 2000; 45:1579–1590.

Latorre-Ossa H, Gennisson JL, De Brosses E, Tanter M. Quantitative imaging of nonlinear shear modulus by combining static elastography and shear wave elastography. IEEE Trans Ultrason Ferroelectr Freq Control 2012;59:833–839.

Lee W-N, Larrat B, Pernot M, Tanter M. Ultrasound elastic tensor imaging: Comparison with MR diffusion tensor imaging in the myocardium. Phys Med Biol 2012a;57:5075–5095.

Lee WN, Pernot M, Couade M, Messas E, Bruneval P, Bel A, Hagege AA, Fink M, Tanter M. Mapping myocardial fiber orientation using echocardiography-based shear wave imaging. IEEE Trans Med Imaging 2012b;31:554–562.

Lerner RM, Huang SR, Parker KJ. "Sonoelasticity" images derived from ultrasound signals in mechanically vibrated tissues. Ultrasound Med Biol 1990;16:231–239.

Ling HY, Zheng YP, Patil SG. Strain dependence of ultrasound speed in bovine articular cartilage under compression in vitro. Ultrasound Med Biol 2007;33:1599–1608.

Litwiller DV, Lee SJ, Kolipaka A, Mariappan YK, Glaser KJ, Pulido JS, Ehman RL. MR elastography of the ex vivo bovine globe. Journal of Magnetic Resonance Imaging 2010;32:44–51.

Litwiller DV, Mariappan YK, Ehman RL. Magnetic resonance elastography. Curr Med Imaging Rev 2012;8:46–55.

Lopez O, Amrami KK, Manduca A, Ehman RL. Characterization of the dynamic shear properties of hyaline cartilage using high-frequency dynamic MR elastography. Magn Reson Med 2008;59:356–564.

Lopez O, Amrami KK, Manduca A, Rossman PJ, Ehman RL. Developments in dynamic MR elastography for in vitro biomechanical assessment of hyaline cartilage under high-frequency cyclical shear. J Magn Reson imaging 2007;25:310–320.

Lorenzen J, Sinkus R, Biesterfeldt M, Adam G. Menstrual-cycle dependence of breast parenchyma elasticity: Estimation with magnetic resonance elastography of breast tissue during the menstrual cycle. Invest Radiol 2003;38:236–240.

Lorenzen J, Sinkus R, Lorenzen M, Dargatz M, Leussler C, Roschmann P, Adam G. MR elastography of the breast: Preliminary clinical results. Rofo 2002;174:830–834.

Luo J, Li RX, Konofagou EE. Pulse wave imaging of the human carotid artery: An in vivo feasibility study. IEEE Trans Ultrasonics Ferroelectr Freq Control 2012;59:174–181.

Luo JW, Fujikura K, Tyrie LS, Tilson MD, Konofagou EE. Pulse wave imaging of normal and aneurysmal abdominal aortas in vivo. IEEE Trans Med Imaging 2009;28:477–486.

Mace E, Cohen I, Montaldo G, Miles R, Fink M, Tanter M. In vivo mapping of brain elasticity in small animals using shear wave imaging. IEEE Trans Med Imaging 2011;30:550–558.

Maleke C, Konofagou EE. Harmonic motion imaging for focused ultrasound (HMIFU): A fully integrated technique for sonication and monitoring of thermal ablation in tissues. Phys Med Biol 2008;53: 1773–1793.

Manduca A, Oliphant TE, Dresner MA, Mahowald JL, Kruse SA, Amromin E, Felmlee JP, Greenleaf JF, Ehman RL. Magnetic resonance elastography: Non-invasive mapping of tissue elasticity. Med Image Anal 2001;5:237–254.

Mannelli L, Godfrey E, Joubert I, Patterson AJ, Graves MJ, Gallagher FA, Lomas DJ. MR elastography: Spleen stiffness measurements in healthy volunteers—preliminary experience. Am J Roentgenol 2010;195:387–392.

Mariappan YK, Glaser KJ, Ehman RL. Magnetic resonance elastography: A review. Clin Anat 2010;23:497–511.

Mariappan YK, Glaser KJ, Hubmayr RD, Manduca A, Ehman RL, McGee KP. MR elastography of human lung parenchyma: Technical development, theoretical modeling and in vivo validation. J Magn Reson Imaging 2011;33:1351–1361.

Mariappan YK, Kolipaka A, Manduca A, Hubmayr RD, Ehman RL, Araoz P, McGee KP. Magnetic resonance elastography of the lung parenchyma in an in situ porcine model with a noninvasive mechanical driver: Correlation of shear stiffness with trans-respiratory system pressures. Magn Reson Med 2012;67:210–217.

McAleavey SA, Menon M, Orszulak J. Shear-modulus estimation by application of spatially-modulated impulsive acoustic radiation force. Ultrasonic Imaging 2007;29:87–104.

McGee KP, Hubmayr RD, Levin D, Ehman RL. Feasibility of quantifying the mechanical properties of lung parenchyma in a small-animal model using H-1 magnetic resonance elastography (MRE). J Magn Reson Imaging 2009;29:838–845.

McKnight AL, Kugel JL, Rossman PJ, Manduca A, Hartmann LC, Ehman RL. MR elastography of breast cancer: Preliminary results. AJR Am J Roentgenol 2002;178:1411–1417.

Mitri FG, Urban MW, Fatemi M, Greenleaf JF. Shearwave dispersion ultrasonic vibrometry (SDUV) for measuring prostate shear stiffness and viscosity: An in vitro pilot study. IEEE Trans Biomed Eng 2011; 58:235–242.

Mol CR, Breddels PA. Ultrasound velocity in muscle. J Acoust Soc Am 1982;71:455–461.

Montaldo G, Tanter M, Bercoff J, Benech N, Fink M. Coherent plane-wave compounding for very high frame rate ultrasonography and transient elastography. IEEE Trans Ultrason Ferroelectr Freq Control 2009;56:489–506.

Muller M, Gennisson JL, Deffieux T, Tanter M, Fink M. Quantitative viscoelasticity mapping of human liver using supersonic shear imaging: Preliminary in vivo feasability study. Ultrasound Med Biol 2009;35:219–229.

Muthupillai R, Lomas DJ, Rossman PJ, Greenleaf JF, Manduca A, Ehman RL. Magnetic resonance elastography by direct visualization of propagating acoustic strain waves. Science 1995;269:1854–1857.

Nedredal GI, Yin M, McKenzie T, Lillegard J, Luebke-Wheeler J, Talwalkar J, Ehman R, Nyberg SL. Portal hypertension correlates with splenic stiffness as measured with MR elastography. J Magn Reson Imaging 2011;34:79–87.

Nenadic IZ, Urban MW, Aristizabal S, Mitchell SA, Humphrey T, Greenleaf JF. On Lamb and Rayleigh wave convergence in viscoelastic tissues. Phys Med Biol 2011a;56:6723–6738.

Nenadic IZ, Urban MW, Bernal M, Greenleaf JF. Phase velocities and attentuations of shear, Lamb, and Rayleigh waves in plate-like tissues submerged in a fluid. J Acoust Soc Am 2011b;130: 3549–3552.

Nenadic IZ, Urban MW, Mitchell SA, Greenleaf JF. Lamb wave dispersion ultrasound vibrometry (LDUV) method for quantifying

mechanical properties of viscoelastic solids. Phys Med Biol 2011c; 56:2245.
Nieminen HJ, Julkunen P, Töyräs J, Jurvelin JS. Ultrasound speed in articular cartilage under mechanical compression. Ultrasound Med Biol 2007;33:1755–1766.
Nightingale K, McAleavey S, Trahey G. Shear-wave generation using acoustic radiation force: In vivo and ex vivo results. Ultrasound Med Biol 2003;29:1715–1723.
Nightingale KR, Palmeri ML, Nightingale RW, Trahey GE. On the feasibility of remote palpation using acoustic radiation force. J Acoust Soc Am 2001;110:625–634.
Nordez A, Gennisson JL, Casari P, Catheline S, Cornu C. Characterization of muscle belly elastic properties during passive stretching using transient elastography. J Biomech 2008;41:2305–2311.
Palmeri ML, Wang MH, Dahl JJ, Frinkley KD, Nightingale KR. Quantifying hepatic shear modulus in vivo using acoustic radiation force. Ultrasound Med Biol 2008;34:546–558.
Parker KJ, Huang SR, Musulin RA, Lerner RM. Tissue response to mechanical vibrations for "sonoelasticity imaging." Ultrasound Med Biol 1990;16:241–246.
Pauly H, Schwan HP. Mechanism of absorption of ultrasound in liver tissue. J Acoust Soc Am 1971;50:692–699.
Pernot M, Couade M, Mateo P, Crozatier B, Fischmeister R, Tanter M. Real-time assessment of myocardial contractility using shear wave imaging. J Am Coll Cardiol 2011;58:65–72.
Pernot M, Fujikura K, Fung-Kee-Fung SD, Konofagou EE. ECG-gated, mechanical and electromechanical wave imaging of cardiovascular tissues in vivo. Ultrasound Med Biol 2007;33:1075–1085.
Provost J, Lee W-N, Fujikura K, Konofagou EE. Imaging the electromechanical activity of the heart in vivo. Proc Natl Acad Sci USA 2011; 108:8565–8570.
Righetti R, Ophir J, Krouskop TA. A method for generating permeability elastograms and Poisson's ratio time-constant elastograms. Ultrasound Med Biol 2005;31:803–816.
Righetti R, Ophir J, Srinivasan S, Krouskop TA. The feasibility of using elastography for imaging the Poisson's ratio in porous media. Ultrasound Med Biol 2004;30:215–228.
Ringleb SI, Bensamoun SF, Chen QS, Manduca A, An KN, Ehman RL. Applications of magnetic resonance elastography to healthy and pathologic skeletal muscle. J Magn Reson Imaging 2007;25: 301–309.
Rouviere O, Yin M, Dresner MA, Rossman PJ, Burgart LJ, Fidler JL, Ehman RL. MR elastography of the liver: Preliminary results. Radiology 2006;240:440–448.
Rubens DJ, Hadley MA, Alam SK, Gao L, Mayer RD, Parker KJ. Sonoelasticity imaging of prostate cancer: In vitro results. Radiology 1995;195:379–383.
Sack I, Beierbach B, Hamhaber U, Klatt D, Braun A. Non-invasive measurement of brain viscoelasticity using magnetic resonance elastography. NMR Biomed 2008;21:265–271.
Sack I, Beierbach B, Wuerfel J, Klatt D, Hamhaber U, Papazoglou S, Martus P, Braun J. The impact of aging and gender on brain viscoelasticity. NeuroImage 2009;46:652–657.
Sandrin L, Fourquet B, Hasquenoph JM, Yon S, Fournier C, Mal F, Christidis C, Ziol M, Poulet B, Kazemi F, Beaugrand M, Palau R. Transient elastography: A new noninvasive method for assessment of hepatic fibrosis. Ultrasound Med Biol 2003;29:1705–1713.
Sandrin L, Tanter M, Catheline S, Fink M. Shear modulus imaging with 2-D transient elastography. IEEE Trans Ultrason Ferroelectr Freq Control 2002a;49:426–435.
Sandrin L, Tanter M, Gennisson JL, Catheline S, Fink M. Shear elasticity probe for soft tissues with 1-D transient elastography. IEEE Trans Ultrason Ferroelectr Freq Control 2002b;49:436–446.
Sarvazyan A, Hall TJ, Urban MW, Fatemi M, Aglyamov SR, Garra B. Elasticity imaging: An emerging branch of medical imaging. An overview. Curr Med Imaging Rev 2011;7:255–282.
Sarvazyan A, Tatarinov A, Sarvazyan N. Ultrasonic assessment of tissue hydration status. Ultrasonics 2005;43:661–671.
Sarvazyan AP. Elastic properties of soft tissues. In: Levy M, Bass HE, Stern RR, (eds). Handbook of elastic properties of solids, liquids and gases. New York: Academic Press; 2001. p. 107–127.
Sarvazyan AP, Hill CR. Physical chemistry of the ultrasound–tissue interaction. In: Hill CR, Bamber JC, ter Haar GR, (eds). Physical principles of medical ultrasonics. West Sussex: Wiley; 2004. pp.
Sarvazyan AP, Lyrchikov AG, Gorelov SE. Dependence of ultrasonic velocity in rabbit liver on water content and structure of the tissue. Ultrasonics 1987;25:244–247.
Sarvazyan AP, Rudenko OV, Swanson SD, Fowlkes JB, Emelianov SY. Shear wave elasticity imaging: A new ultrasonic technology of medical diagnostics. Ultrasound Med Biol 1998;24:1419–1435.
Sinkus R, Daire J-L, Vilgrain V, Van Beers BE. Elasticity imaging via MRI: Basics, overcoming the waveguide limit, and clinical liver results. Curr Med Imaging Rev 2012;8:56–63.
Sinkus R, Siegmann K, Xydeas T, Tanter M, Claussen C, Fink M. MR elastography of breast lesions: Understanding the solid/liquid duality can improve the specificity of contrast-enhanced MR mammography. Magn Reson Med 2007;58:1135–1144.
Sinkus R, Tanter M, Catheline S, Lorenzen J, Kuhl C, Sondermann E, Fink M. Imaging anisotropic and viscous properties of breast tissue by magnetic resonance-elastography. Magn Reson Med 2005a;53: 372–387.
Sinkus R, Tanter M, Xydeas T, Catheline S, Bercoff J, Fink M. Viscoelastic shear properties of in vivo breast lesions measured by MR elastography. Magn Reson Imaging 2005b;23:159–165.
Song P. Ultrasound transient shear wave elasticity imaging for tendon tissue. *Agricultural and Biological Systems Engineering* Lincoln, NE: University of Nebraska 2010;1–111.
Sosnovik DE, Baldwin SL, Lewis SH, Holland MR, Miller JG. Transmural variation of myocardial attenuation measured with a clinical imager. Ultrasound Med Biol 2001;27:1643–1650.
Stebbing J, Farouk L, Panos G, Anderson M, Jiao LR, Mandalia S, Bower M, Gazzard B, Nelson M. A meta-analysis of transient elastography for the detection of hepatic fibrosis. J Clin Gastroenterol 2010;44:214–219.
Stewart EA, Taran FA, Chen J, Gostout BS, Woodrum DA, Felmlee JP, Ehman RL. Magnetic resonance elastography of uterine leiomyomas: A feasibility study. Fertil Steril 2011;95:281–284.
Stock KF, Klein BS, Vo Cong MT, Sarkar O, Römisch M, Regenbogen C, Büttner M, Schuster T, Matevossian E, Amann K, Clevert DA, Heemann U, Küchle C. ARFI-based tissue elasticity quantification in comparison to histology for the diagnosis of renal transplant fibrosis. Clin Hemorheol Microcirc 2010;46:139–148.
Stolz M, Raiteri R, Daniels AU, VanLandingham MR, Baschong W, Aebi U. Dynamic elastic modulus of porcine articular cartilage determined at two different levels of tissue organization by indentation-type atomic force microscopy. Biophys J 2004;86: 3269–3283.
Sugimoto T, Ueha S, Itoh K. Tissue hardness measurement using the radiation force of focused ultrasound. 1990 IEEE International Ultrasonics Symposium 1990;1377–1380.
Syversveen T, Brabrand K, Midtvedt K, Strøm EH, Hartmann A, Jakobsen JA, Berstad AE. Assessment of renal allograft fibrosis by acoustic radiation force impulse quantification: A pilot study. Transplant Int 2011;24:100–105.
Talwalkar JA, Yin M, Venkatesh S, Rossman PJ, Grimm RC, Manduca A, Romano A, Kamath PS, Ehman RL. Feasibility of in vivo MR elastographic splenic stiffness measurements in the assessment of portal hypertension. Am J Roentgenol 2009;193: 122–127.
Tanter M, Bercoff J, Athanasiou A, Deffieux T, Gennisson JL, Montaldo G, Muller M, Tardivon A, Fink M. Quantitative assessment of breast lesion viscoelasticity: Initial clinical results using supersonic shear imaging. Ultrasound Med Biol 2008;34: 1373–1386.
Tanter M, Touboul D, Gennisson JL, Bercoff J, Fink M. High-resolution quantitative imaging of cornea elasticity using supersonic shear imaging. IEEE Trans Med Imaging 2009;28:1881–1893.
Uffmann K, Maderwald S, Ajaj W, Galban CG, Mateiescu S, Quick HH, Ladd ME. In vivo elasticity measurements of extremity skeletal muscle with MR elastography. NMR Biomed 2004;17:181–190.
Urban MW, Alizad A, Aquino W, Greenleaf JF, Fatemi M. A review of vibro-acoustography and its applications in medicine. Curr Med Imaging Rev 2011;7:350–359.

Urban MW, Chen S, Fatemi M. A review of shearwave dispersion ultrasound vibrometry (SDUV) and its applications. Curr Med Imaging Rev 2012;8:27–36.

Urban MW, Chen S, Greenleaf JF. Error in estimates of tissue material properties from shear wave dispersion ultrasound vibrometry. IEEE Trans Ultrason Ferroelectr Freq Control 2009;56:748–758.

Urban MW, Greenleaf JF. A Kramers–Kronig-based quality factor for shear wave propagation in soft tissue. Phys Med Biol 2009;54: 5919–5933.

Vappou J, Luo JW, Konofagou EE. Pulse wave imaging for noninvasive and quantitative measurement of arterial stiffness in vivo. Am J Hypertens 2010;23:393–398.

Vappou J, Maleke C, Konofagou EE. Quantitative viscoelastic parameters measured by harmonic motion imaging. Phys Med Biol 2009; 54:3579–3594.

Wang SG, Lee WN, Provost J, Luo JW, Konofagou EE. A composite high-frame-rate system for clinical cardiovascular imaging. IEEE Trans Ultrason Ferroelectr Freq Control 2008; 55:2221–2233.

Wu Z, Taylor LS, Rubens DJ, Parker KJ. Sonoelastographic imaging of interference patterns for estimation of the shear velocity of homogeneous biomaterials. Phys Med Biol 2004;49:911–922.

Yamakoshi Y, Sato J, Sato T. Ultrasonic imaging of internal vibration of soft tissue under forced vibration. IEEE Trans Ultrason Ferroelectr Freq Control 1990;37:45–53.

Yasar TK, Royston TJ, Magin RL. Wideband MR elastography for viscoelasticity model identification. Magn Reson Med 2012 September 21; http://dx.doi.org/10.1002/mrm.24495 [Epub ahead of print].

Zhang J, Green MA, Sinkus R, Bilston LE. Viscoelastic properties of human cerebellum using magnetic resonance elastography. J Biomech 2011a;44:1909–1913.

Zhang X, Kinnick RR, Fatemi M, Greenleaf JF. Noninvasive method for estimation of complex elastic modulus of arterial vessels. IEEE Trans Ultrason Ferroelectr Freq Control 2005;52: 642–652.

Zhang X, Osborn TG, Pittelkow MR, Qiang B, Kinnick RR, Greenleaf JF. Quantitative assessment of scleroderma by surface wave technique. Med Eng Phys 2011b;33:31–37.

Zhang X, Qiang B, Hubmayr RD, Urban MW, Kinnick R, Greenleaf JF. Noninvasive ultrasound image guided surface wave method for measuring the wave speed and estimating the elasticity of lungs: A feasibility study. Ultrasonics 2011c;51:289–295.